Tumor-associated macrophages and macrophage-related immune checkpoint expression in sarcomas

Amanda R. Dancsok , Dongxia Gao , Anna F. Lee , Sonja Eriksson Steigen , Jean-Yves Blay , David M. Thomas , Robert G. Maki , Torsten O. Nielsen & Elizabeth G. Demicco

Taylor & Francis
Taylor & Francis Group

ORIGINAL RESEARCH

Tumor-associated macrophages and macrophage-related immune checkpoint expression in sarcomas

Amanda R. Dancsok[a], Dongxia Gao[a], Anna F. Lee[a], Sonja Eriksson Steigen[b], Jean-Yves Blay [c], David M. Thomas[d], Robert G. Maki[e]*, Torsten O. Nielsen[a], and Elizabeth G. Demicco[f]

[a]Department of Pathology and Laboratory Medicine, Vancouver Coastal Health Research Institute and University of British Columbia, Vancouver, BC, Canada; [b]Clinical Pathology and Institute of Medical Biology, Faculty of Health Sciences, University Hospital of Northern Norway, Tromsø, Norway; [c]Department of Medical Oncology, Centre Léon Bérard and University Claude Bernard Lyon 1, Lyon, France; [d]The Kinghorn Cancer Centre and Cancer Theme, Garvan Institute of Medical Research, Darlinghurst, Australia; [e]Northwell Health Monter Cancer Center and Cold Spring Harbor Laboratory, Lake Success, NY, USA; [f]Department of Pathology and Laboratory Medicine, Mount Sinai Hospital and Department of Laboratory Medicine and Pathobiology, University of Toronto, Toronto, ON, Canada

ABSTRACT
Early trials for immune checkpoint inhibitors in sarcomas have delivered mixed results, and efforts to improve outcomes now look to combinatorial strategies with novel immunotherapeutics, including some that target macrophages. To enhance our understanding of the sarcoma immune landscape, we quantified and characterized tumor-associated macrophage infiltration and expression of the targetable macrophage-related immune checkpoint CD47/SIRPα across sarcoma types. We surveyed immunohistochemical expression of CD68, CD163, CD47, and SIRPα in tissue microarrays of 1242 sarcoma specimens (spanning 24 types). Non-translocation sarcomas, particularly undifferentiated pleomorphic sarcoma and dedifferentiated liposarcoma, had significantly higher counts of both CD68+ and CD163 + macrophages than translocation-associated sarcomas. Across nearly all sarcoma types, macrophages outnumbered tumor-infiltrating lymphocytes and CD163+ (M2-like) macrophages outnumbered CD68+ (M1-like) macrophages. These findings were supported by data from The Cancer Genome Atlas, which showed a correlation between increasing macrophage contributions to immune infiltration and several measures of DNA damage. CD47 expression was bimodal, with most cases showing either 0% or >90% tumor cell staining, and the highest CD47 scores were observed in chordoma, angiosarcoma, and pleomorphic liposarcoma. SIRPα scores correlated well with CD47 expression. Given the predominance of macrophage infiltrates over tumor-infiltrating lymphocytes, the bias toward M2-like (immunosuppressive) macrophage polarization, and the generally high scores for CD47 and SIRPα, macrophage-focused immunomodulatory agents, such as CD47 or IDO-1 inhibitors, may be particularly worthwhile to pursue in sarcoma patients, alone or in combination with lymphocyte-focused agents.

Introduction

Sarcomas are a diverse group of mesenchymal malignancies, with over 50 biologically and clinically distinct types described by the World Health Organization.[1] Unfortunately, due to the rarity of some sarcomas, clinical trials often lump together different sarcoma types to improve accrual and power. This practice may disguise real clinical responses to investigational agents, due to the confounding presence of sarcoma types with very different biology.

Sarcomas were the first cancers to be successfully treated by immunotherapy (Coley's bacterial toxins in 1891),[2] leading to great interest in the application of modern cancer immunotherapy to sarcomas. Several immune checkpoint inhibitors have been investigated in sarcomas,[3-5] but due to low numbers for any individual type, it has been difficult to glean any conclusive findings. Trials of immune checkpoint inhibitors in other cancers are beginning to reveal high levels of

therapeutic resistance by immune escape mechanisms, including activation of other (untargeted) immune checkpoints.[6] This is leading to the increasing use of combinatorial therapeutic inhibition of two or more immune checkpoints, including some macrophage-related checkpoints, such as the CD47/SIRPα "don't eat me" signal. To guide design of these combinatorial studies, particularly in a group as heterogeneous as sarcomas, it is critical to have a detailed, type-specific understanding of their immune microenvironments.

Tumor-associated macrophages can affect tumor cell proliferation, stromal formation and dissolution, vascularization, and both pro- and anti-neoplastic inflammation.[7] Tumor-associated macrophages are conventionally divided into two simplified subgroups: M1-like (classically activated by IFNγ, pro-inflammatory, and involved in tumor killing via complement-mediated phagocytosis),[8-10] and M2-like (alternatively activated, anti-inflammatory, and involved in tissue repair

and resolution of inflammation).[8] Prior to polarization, macrophages first exist as M0 (uncommitted) macrophages; cytokine stimuli then largely determine the subsequent direction of polarization.[11,12] This polarization is plastic, and macrophages can switch polarization in response to further external stimuli including IFNγ[13] and IL-10.[14]

High levels of tumor-associated macrophages are generally a poor prognostic factor in most cancer types,[15,16] and macrophages were identified in 90% (45/50) of tumors in a study of sarcomas of various types (14 GIST, 5 synovial sarcoma, 4 leiomyosarcoma, and 1–3 cases of 18 other types),[17] as well as in both alveolar and embryonal rhabdomyosarcoma.[18] In The Cancer Genome Atlas (TCGA) study of 206 adult soft tissue sarcomas, macrophage scores derived from gene expression signatures[19,20] were highest among dedifferentiated liposarcoma, myxofibrosarcoma, and UPS, but lower in synovial sarcoma. In leiomyosarcoma, two studies demonstrated an association between higher density of CD68+ or CD163 + macrophage infiltration and poorer clinical outcomes,[21,22] perhaps explaining the poor outcomes for leiomyosarcomas in lymphocyte-based adaptive immune checkpoint inhibitor clinical trials.[3-5,23]

CD47 is a ubiquitously expressed cell-surface protein that protects viable erythrocytes from phagocytosis, sometimes referred to as the "don't eat me" signal.[24-30] In cancer, CD47 can be over-expressed to evade phagocyte-mediated anti-tumor immunity via interaction with SIRPα (signal-regulatory protein alpha), a cell-surface receptor expressed by macrophages and dendritic cells.[31] Anti-CD47 monoclonal antibodies have impressive activity in mouse xenograft models,[32-39] leading to the opening of clinical trials targeting the CD47/SIRPα axis. In phase 1 studies targeting CD47/SIRPα signaling, encouraging responses were seen in both lymphoma and advanced solid tumors.[39-42] Overexpression of CD47 has been observed across most cancers,[32-36,43-45] including in osteosarcoma,[46] but has never been systematically examined in soft tissue sarcomas.

In this study, we assessed a wide array of sarcomas (1242 cases, over 27 sarcoma types) to determine type-specific expression patterns of M1-like and M2-like tumor-associated macrophages and the CD47/SIRPα immune checkpoint, and their associations with clinical parameters and survival.

Materials and methods

Patient tumor samples

From the University of British Columbia Genetic Pathology Evaluation Center (Vancouver, BC, Canada), 14 formalin-fixed, paraffin-embedded tissue microarrays (TMAs) were included: TMA 01–003 (synovial sarcoma and differential diagnoses, 82 cases in duplicate);[47] TMA 03–008 (chondroid tumors, 121 cases in duplicate);[48] TMA 06-001E (gastrointestinal stromal tumors, 129 cases in duplicate);[49] TMA 06–007 (myxoid liposarcomas, 69 cases in triplicate);[50] TMA 09–006 (epithelioid sarcoma and differential diagnoses, 53 cases in duplicate);[51] TMA 10–004 (28 chordomas, in duplicate); TMA 10–009 (8 alveolar soft part sarcomas, 2 alveolar rhabdomyosarcomas, 2 desmoplastic small round

cell tumors, in triplicate);[51] TMA 12–004 (BCL2-positive tumors, 35 cases in triplicate);[52] TMA 12–005 (pediatric spindle cell lesions, 134 cases in duplicate);[52] TMA 12–006 (translocation-associated sarcomas, 10 cases in duplicate);[52] TMA 12–010 (5 dedifferentiated liposarcomas and 5 undifferentiated pleomorphic sarcomas, in duplicate);[52] TMA 14–006 (4 myxoid liposarcomas, 3 myxofibrosarcomas, 3 chondrosarcomas, 1 synovial sarcoma, 1 malignant peripheral nerve sheath tumor, in duplicate);[53] TMA 14–007 (dedifferentiated liposarcomas with well-differentiated areas, both components for 57 cases in duplicate);[54] and TMA MPNST (malignant peripheral nerve sheath tumor and differential diagnoses, 176 cases in duplicate).[55] From Mount Sinai Hospital (New York, NY, USA), four TMAs were included: MSH-OSa (osteosarcomas, 280 cases in duplicate); MSH-SS (synovial sarcomas, 70 cases in duplicate); MSH-SFT (solitary fibrous tumors, 140 cases in duplicate);[56] and MSH-UPS (74 undifferentiated pleomorphic sarcomas, 52 myxofibrosarcomas, 18 leiomyosarcomas, 13 dedifferentiated liposarcomas, 9 dermatofibrosarcoma protuberans, and differential diagnoses; 210 cases total in duplicate).

Tissue microarray preparation

All tissue specimens were derived from surgical resection specimens from Mount Sinai Hospital, New York, NY (MSH TMAs), 20 centers throughout Norway (TMA 06–001), BC Children's Hospital (TMA 12–005), or Vancouver General Hospital, Vancouver, BC (all other TMAs). Cores with a diameter of 1.0 mm (TMA 14–007, all MSH TMAs) or 0.6 mm (all other TMAs) were extracted from representative viable tumor tissue, as identified by a bone and soft tissue subspecialty pathologist (AF Lee, TO Nielsen, EG Demicco). TMAs were cut to 4-μm-thick sections, mounted to Fisherbrand™ Superfrost™ Plus charged glass slides (Thermo Fisher Scientific Inc, Waltham, MA), and incubated for 1 h at 60°C.

Immunohistochemistry

Immunohistochemical staining was performed on serial TMA sections, which were cut in parallel batches and processed immediately. All antibodies were applied using the Ventana DISCOVERY® ULTRA semi-automated staining system (Ventana Medical Systems Inc., Tucson, AZ), as described previously.[54] Briefly, heat-induced antigen retrieval was performed using the standard Cell Conditioning 1 (CC1, Ventana) protocol. Slides were incubated with primary antibodies (described in Table S1) in DISCOVERY antibody diluent (Ventana) for 2 h at room temperature. For CD68, CD47, and SIRPα, slides were incubated for 16 min at 37°C in DISCOVERY Universal secondary antibody (Ventana), and chromogen visualization was performed by DAB map detection (Ventana). For CD163, slides were incubated for 2 h at room temperature with the UltraMap anti-mouse secondary antibody (Ventana) and visualized using the UltraMap DAB Kit (Ventana). PDL1 staining methodology was previously reported.[57]

All slides were counterstained with hematoxylin and mounted. Digital images of immunostained tissue microarrays

were acquired using the Olympus BLISS high-definition virtual microscope and slide scanner (Olympus Life Science Solutions: Bacus Laboratories, Lombard, IL, USA) or the Aperio digital pathology slide scanner (Leica Biosystems, Wetzlar, Germany).

Histological scoring

Scoring was performed by pathologists experienced in scoring biomarkers in bone and soft tissue tumors (EG Demicco, D Gao). All immunohistochemical markers were scored for cytomembranous positivity. Replicate cores were scored separately, with the pathologist blinded to replicate status and final histological diagnosis. Macrophage biomarkers (CD68, CD163, SIRPα) were scored by counting the number of positive-staining macrophages per TMA core (Figure 1(a,b,d)) divided by the area of the core to yield a value for macrophages/mm^2, up to 2000/mm^2 (scores above this threshold were marked as 2000/mm^2). CD47 was scored as the percentage of positive-staining sarcoma tumor cells (Figure 1(c)). CD47 staining intensity was also scored, but excluded from analyses due to mainly uniform (saturated) intensity across positive samples. As previously reported, tumor-infiltrating lymphocytes (TILs) were counted directly from hematoxylin and eosin stained slides and similarly expressed as an absolute count per mm^2, and PDL1 was quantitated both on tumor cells and inflammatory cells.[57]

TCGA data analysis

Data on relative proportions of macrophages and macrophage subsets (M0, M1, M2) and measures of DNA damage was extracted from published data (Thorsson et al. (2018),[58] Supplemental Table 1, PanImmune Feature Matrix of Immune Characteristics; https://www.cell.com/cms/10.1016/j.immuni.2018.03.023/attachment/22b1df93-e78b-40b9-bceb-2e69aa3f55d2/mmc2.xlsx), and analyzed according to the 6 sarcoma types defined in the TGCA sarcoma analysis: dedifferentiated liposarcoma (n = 50), myxofibrosarcoma (n = 17), undifferentiated pleomorphic sarcoma (n = 44), leiomyosarcoma (n = 80), malignant peripheral nerve sheath tumor (n = 5), and synovial sarcoma (n = 10).[20] Data on macrophages and polarized subsets of macrophages are represented as a percent of the total immune infiltrate (leukocyte fraction) in a given case and do not reflect absolute differences between cases. DNA damage measures were defined per Thorsson et al.[58] as follows: Intratumoral heterogeneity was assessed as subclonal genome fraction less the percent of the tumor genome not represented by the plurality clone; Homologous recombination deficiency (HRD) score summed three variables: (1) number of regions of>15 Mb with loss of heterozygosity, (2) breaks between adjacent segments of >10 Mb, and (3) allelic imbalances in subtelomeric regions; Aneuploidy score was defined as the sum total of amplified or deleted chromosome arms. Segments altered represent the total number of altered chromosome segments in a sample. The non-silent mutation rate, and predicted single nucleotide and indel neoantigens (pMHCs), were likewise taken as calculated by Thorsson et al.[58]

Statistical analysis

Data analysis was performed using IBM® SPSS® statistics software (version 26). An Independent Samples Kruskal–Wallis one-way ANOVA test was used to assess the
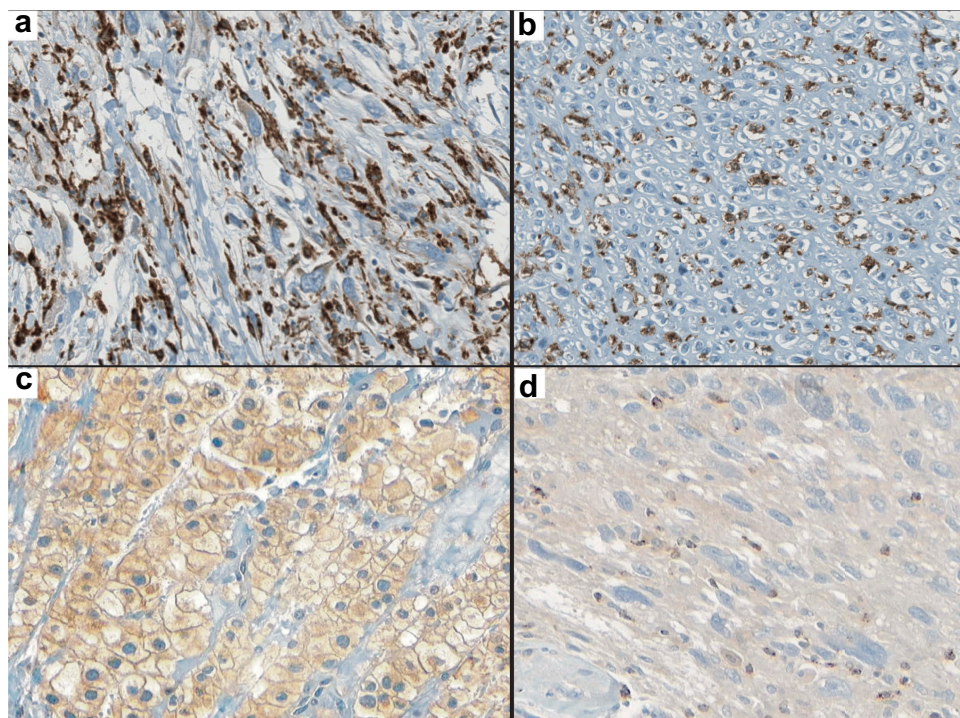

Figure 1. Immunohistochemical staining of macrophage and checkpoint biomarkers in sarcoma tissues. (a) CD68 (KP1 antibody), dedifferentiated liposarcoma; (b) CD163 (10D6), osteosarcoma; (c) CD47 (B6H12), chordoma; (d) SIRPα (A-1), dedifferentiated liposarcoma.

Table 1. Clinical and histopathological characteristics of sarcoma samples used in this study.

Sarcoma Types	Total cases	Patients with clinical data		Patients with clinical data
	n	n		n
Translocation-Associated	**403**	**300**	**FNCLCC grade**	
Synovial sarcoma	140	104	1	95
Solitary fibrous tumor	113	100	2	209
Myxoid liposarcoma	40	35	3	198
Dermatofibrosarcoma protuberans	33	11	Unknown/na	257
Ewing sarcoma	21	15	**Neoadjuvant treatment**	
Alveolar rhabdomyosarcoma	10	6	None	396
LGFMS	9	8	Chemotherapy	97
Alveolar soft part sarcoma	8	4	Radiation therapy	40
Clear cell sarcoma	7	5	CTRT	16
EMC	6	4	Unknown	210
Congenital fibrosarcoma	4	4	**Adjuvant treatment**	
Other*	12	4	None	304
Non-translocation	**839**	**459**	Chemotherapy	82
Osteosarcoma	247	162	Radiation therapy	60
GIST	129	0	CTRT	15
MPNST	77	18	Unknown	298
UPS	72	53	**Overall survival**	
Dedifferentiated liposarcoma	62	58	Alive	437
Well differentiated liposarcoma	59	7	Died	262
Chondrosarcoma***	62	58	Unknown	60
Myxofibrosarcoma	41	33	**Progression-free survival**	
Chordoma	28	23	Alive, NED	288
Leiomyosarcoma	20	19	Progression/died	310
Embryonal rhabdomyosarcoma	12	8	Unknown	161
Epithelioid sarcoma	9	8		
Pleomorphic liposarcoma	7	0		
Angiosarcoma	4	3		
Intimal sarcoma	4	3		
Other**	6	6		
Total	**1242**	**759**		

"Sarcoma Types" column describes all cases in our dataset (N = 1242) as well as those patients for which clinical data is available (n = 759); "Clinical Parameters" column describes only the subset of patients for which clinical data is available. Abbreviations: CTRT, chemoradiation therapy; EMC, extraskeletal myxoid chondrosarcoma; FNCLCC, Fédération Nationale des Centers de Lutte Contre le Cancer; GIST, gastro-intestinal stromal tumor; LGFMS, low grade fibromyxoid sarcoma; MPNST, malignant peripheral nerve sheath tumor; na, not applicable; NED, no evidence of disease; UPS, undifferentiated pleomorphic sarcoma. *Other translocation sarcomas include types with fewer than four cases each (mesenchymal chondrosarcoma, n = 3; angiomatoid fibrous histiocytoma, n = 2; desmoplastic small round cell sarcoma, n = 2; epithelioid hemangioendothelioma, n = 2; sclerosing epithelioid fibrosarcoma, n = 1; malignant myoepithelioma, n = 1, phosphaturic mesenchymal tumor, n = 1). **Other non-translocation sarcomas include adult fibrosarcoma, n = 1, sarcoma NOS, n = 4; radiation-induced sarcoma, n = 1. ***Conventional chondrosarcoma includes four dedifferentiated chondrosarcoma.

differences in scoring between histological types. Categories were compared pairwise, and significance values were adjusted using the Bonferroni correction for multiple comparisons. Correlations between clinicopathologic features and immunohistochemical scores were assessed using an independent sample Kruskal–Wallis 1-way ANOVA, Mann–Whitney U test, Chi-squared, Fisher exact test, or Spearman rank correlation coefficient (r_S), as appropriate. Multiple comparisons corrections were applied for clinico-pathological-immunoprofile correlations using the Bonferroni method. Correlations between scores for different biomarkers and correlation between TCGA macrophage signatures and DNA damage, and between individual immunohistochemical markers were assessed using the Spearman rank correlation coefficient. In order to include cases with very low (0) levels of infiltrating immune cells and compare relative proportions between CD68+ macrophages, CD163+ macrophages, and tumor-infiltrating lymphocytes, the counted number of positive cells/mm^2 was increased by one for all cases prior to calculating the ratio (adjusted CD68:TIL ratio/adjusted CD163: CD68 ratio). Survival correlates for overall survival (OS) and progression-free survival (PFS) among all non-translocation or translocation-associated sarcomas were evaluated using a Cox proportional hazards multiple regression analysis to generate hazard ratios and corresponding 95% confidence intervals. Univariable Cox proportional hazards models were used to assess prognostic significance of macrophage and clinicopathologic features in individual sarcoma types. Statistically significant differences were defined as $p < .05$.

Ethics

Human tissue accessions for these studies were reviewed and approved by the British Columbia Cancer Agency and the Mount Sinai Hospital research ethics boards.

Results

Quantification of tumor-associated macrophages in the study set

Surgical resection specimens from 1242 sarcomas (24 histo-types with at least 4 cases for analysis, Table 1) and 252 benign bone or soft-tissue tumors (Table S2) were available
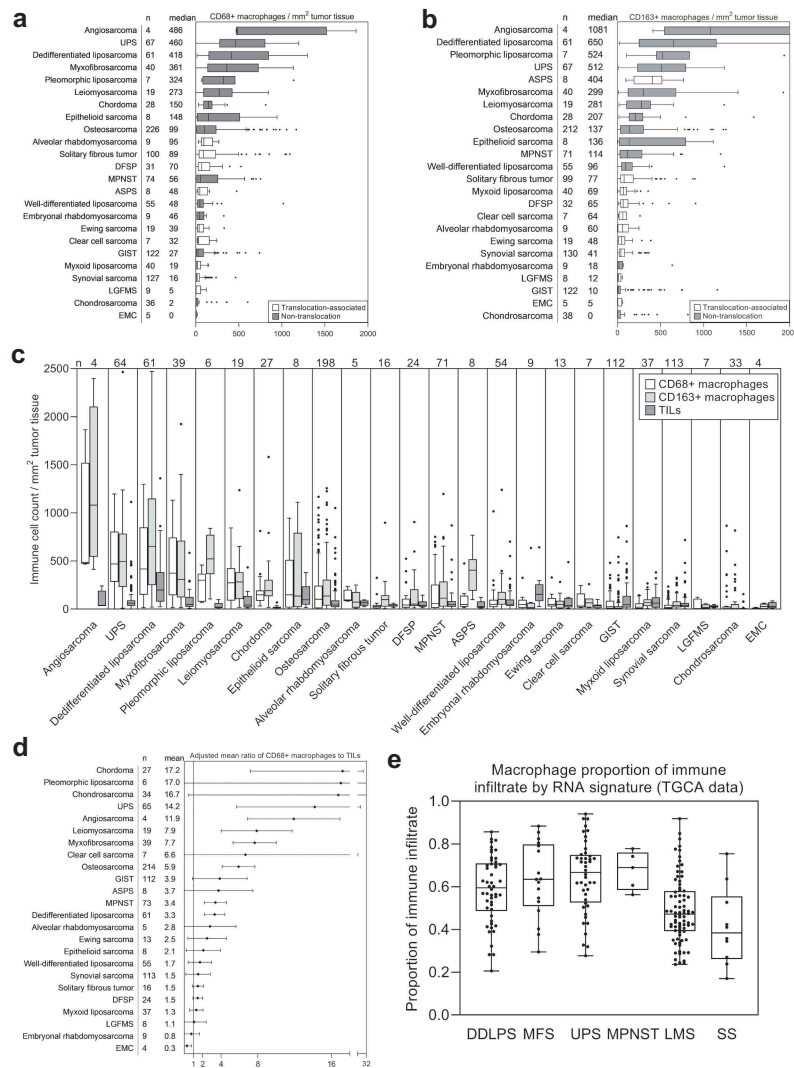
Figure 2. Quantification of tumor-associated macrophages in sarcomas. (a) Boxplots depicting comparative counts of CD68+ macrophages across sarcoma types. Boxes represent the first through third quartiles, vertical line indicates median, and whiskers indicate range. Extreme outliers are indicated as dots. (b) Boxplots depicting comparative counts of CD163+ macrophages across sarcoma types. (c) Boxplots depicting comparative counts of CD68+ macrophages (white), CD163 + macrophages (light gray), and tumor-infiltrating lymphocytes (TILs; dark gray) across sarcoma histotypes. (d) Adjusted mean ratio of CD68/TIL, based on counts of positive-staining immune cells per mm2 tumor tissue, scored from tissue microarray cores. Error bars represent 95% confidence interval of the mean. In order to avoid dividing by zero, all counts were adjusted by adding 1/mm² prior to calculating ratio. (e) Boxplot illustrating proportion of tumor-immune infiltrates represented by macrophages using mRNA expression signatures calculated on TCGA sarcoma types by Thorsson et al. (2018). Dots indicate individual tumor specimens. Abbreviations: ASPS, Alveolar soft part sarcoma, DDLPS, dedifferentiated liposarcoma; DFSP, dermatofibrosarcoma protuberans; EMC, extraskeletal myxoid chondrosarcoma; GIST, gastrointestinal stromal tumor; LGFMS, low grade fibromyxoid sarcoma; LMS, leiomyosarcoma; MFS, myxofibrosarcoma; MPNST, malignant peripheral nerve sheath tumor; SS, synovial sarcoma; UPS, undifferentiated pleomorphic sarcoma.

for evaluation. Clinical data was available for 759 sarcoma patients (Table 1, Table S3).

We quantified tumor-associated macrophages using immunohistochemical markers CD68 (preferentially staining M1-like macrophages with some M2 overlap) and CD163 (preferentially staining M2-like macrophages). Pleomorphic sarcoma types demonstrated the highest counts of both CD68+ and CD163 + macrophages (Figure 2(a,b)), particularly undifferentiated pleomorphic sarcoma (median CD68 = 460/mm², CD163 = 512/ mm²), dedifferentiated liposarcoma (median CD68 = 418/mm², CD163 = 650/mm²), myxofibrosarcoma (median CD68 = 361/ mm², CD163 = 299/mm²), and leiomyosarcoma (median CD68 = 273/mm², CD163 = 281/mm²). Angiosarcomas had the highest counts for both macrophage markers (CD68 = 486/mm²,

CD163 = 1081/mm²), but these counts were scored from only four patients (Figure 2(a,b)). As a group, sarcomas driven by mutations and/or copy-number alterations (non-translocation-associated sarcomas) had significantly higher ($p < .001$) macrophage counts (median CD68 = 105/mm², CD163 = 139/mm²) than did the translocation-associated sarcomas (median CD68 = 36/mm², CD163 = 59/mm²) or benign mesenchymal tumors (median CD68 = 18/mm², CD163 = 38/mm²) (Figure S1A). Translocation-associated sarcomas as a group showed no significant difference in macrophage infiltrate counts when compared to benign mesenchymal tumors; however, alveolar soft part sarcomas had some of the highest CD163+ macrophage densities, with a median count of 404/mm² (Figure 2(b)). Across the sample set, there was a strong correlation between density of CD68+ and CD163

+ macrophages ($r_S = 0.75$, $p < .001$), possibly reflecting their partial phenotypic overlap.

The degree of CD68+ macrophage infiltrates, but not CD163+ expression, was associated with several clinicopathologic features in exploratory analyses (Table S4A and S4B). Patient age positively correlated with CD68+ macrophage infiltrates in myxofibrosarcoma ($r_s = 0.49$, $p = .017$), and negatively correlated with CD68+ macrophage infiltrates in solitary fibrous tumor ($r_s = - 0.31$, $p = .021$). CD68+ macrophage infiltrates were significantly denser in high grade myxofibrosarcomas compared to low-grade tumors. Macrophage infiltrates showed inconsistent increases or decreases across tumor types in response to neoadjuvant therapy or recurrence.

Across nearly all sarcoma types investigated, macrophage infiltrates outnumbered tumor-infiltrating lymphocytes (Figure 2(c)).[57] Macrophage predominance was particularly evident among the non-translocation sarcomas, with over ten-fold adjusted CD68:TIL ratios for chordoma, pleomorphic liposarcoma, chondrosarcoma, undifferentiated pleomorphic sarcoma, and angiosarcoma (Figure 2(d)). Non-translocation sarcomas had a significantly higher adjusted CD68:TIL ratio (mean: 6.7, 95% CI: 5.3–8.0) than was observed among the translocation-associated sarcomas (mean: 1.8, 95% CI: 1.3–2.3)($p < .001$, Figure S1B).

We compared our immunohistochemical quantitation of macrophage density with the macrophage signatures calculated from mRNA expression data for sarcomas analyzed in The Cancer Genome Atlas (TCGA).[20] Similar to our own findings, the TCGA data showed that the highest macrophage signature expression was found in dedifferentiated liposarcoma and undifferentiated pleomorphic sarcoma/myxofibrosarcoma. Leiomyosarcoma had the lowest macrophage signatures among the non-translocation sarcomas evaluated, and synovial sarcoma had the lowest overall macrophage signature expression.[20] We further investigated the relative proportion of macrophages in sarcoma immune infiltrates – calculated from published gene expression signatures[58] – and found that, in dedifferentiated liposarcoma, myxofibrosarcoma, undifferentiated pleomorphic sarcoma, and malignant peripheral nerve sheath tumor, macrophages were more likely to comprise over half of the total immune infiltrates, while in leiomyosarcoma and synovial sarcomas, the median contribution of macrophages to the overall immune infiltrate was less than 50% (Figure 2(e)). These findings at the RNA level support the validity of our immunohistochemical quantitation and relative macrophage:TIL ratios in sarcomas.

Macrophage polarization

Using CD163 as a marker of M2-like (anti-inflammatory) macrophages and CD68 as a marker of M1-like (pro-inflammatory) macrophages,[59] we observed that sarcomas tend to have a higher proportion of M2-like than M1-like macrophages (Figure 3(a)), particularly undifferentiated pleomorphic sarcoma (adjusted mean CD163/CD68 = 20.7, n = 65) and leiomyosarcoma (adjusted mean CD163/CD68 = 17.4, n = 19). The M2-like:M1-like ratio was relatively balanced in epithelioid sarcoma, clear cell sarcoma, and both embryonal and alveolar rhabdomyosarcomas (Figure 3(a)).

Similarly, within the sarcoma types analyzed by the TCGA using gene expression signatures,[58] M2 macrophages represented a larger proportion of the total immune infiltrate than either M0- or M1- polarized macrophages (Figure S2). The median calculated M2:(M0+ M1) ratio was higher in the non-translocation sarcomas, ranging from 2.1 (malignant peripheral nerve sheath tumor) to 8.6 (dedifferentiated liposarcoma), whereas synovial sarcoma tended to have more uncommitted M0 macrophages than M2 (median ratio M2:(M0+ M1) = 0.7).

In order to determine if macrophage infiltrates might be related to the extent of genomic alterations in sarcoma, we calculated Spearman rank correlation coefficients between macrophage proportion and measures of genomic complexity in four major non-translocation sarcoma types (dedifferentiated liposarcoma (n = 50), leiomyosarcoma (n = 80), undifferentiated pleomorphic sarcoma (n = 44), and myxofibrosarcoma (n = 17)) using data from Thorsson et al.[58]

Overall, intratumoral heterogeneity showed a significant positive correlation with increasing proportions of macrophages in the immune microenvironment ($p < .05$), as did measures representing armlevel chromosomal alterations (aneuploidy score), focal chromosomal copy number alterations (number of chromosomal segments altered), and homologous recombination defects. No significant changes in relative macrophage proportion were observed based on small nucleotide alterations (non-silent mutation rate or number of predicted neoantigens) (Figure 3(b)). Among individual tumor types, only leiomyosarcoma showed strong correlations between macrophage infiltrates and chromosomal alterations. When the DNA damage scores were correlated with individual proportions of M0-, M1-, and M2- polarized macrophages (Figure 3(c–e)), it was found that the increasing proportions of macrophages in cases with higher intratumoral heterogeneity, increased copy number alterations, or more homologous recombination defects were attributable to increased M2 macrophages infiltrates in these cases (Figure 3(e)); however, leiomyosarcomas also showed increased proportions of M0 macrophages in cases with more frequent copy number alterations and homologous recombination defects (Figure 3(c)). While the M1:M2 ratio weakly correlated with measures of DNA damage, these findings did not reach significance in most sarcomas (Figure 3(f)).

Macrophage-related immune checkpoint: CD47/SIRPα

We next surveyed our sarcoma tissues for the tumor-cell-expressed immune checkpoint CD47 and the corresponding macrophage-expressed receptor SIRPα (Figure 4(a)). The distribution of CD47 scores was distinctly bimodal across the full sample set, with most tissue microarray cores staining at either 0% or ≥90% positive tumor cells (47.5% and 31.5% of total cases, respectively; Figure 4(b)). Over half (52.5%) of the evaluated sarcomas expressed at least focal CD47, and expression varied widely among sarcoma types. Sarcoma types with consistently infrequent CD47 expression included undifferentiated pleomorphic sarcoma (82% of cases negative for CD47), leiomyosarcoma (78% of cases negative for CD47), and Ewing
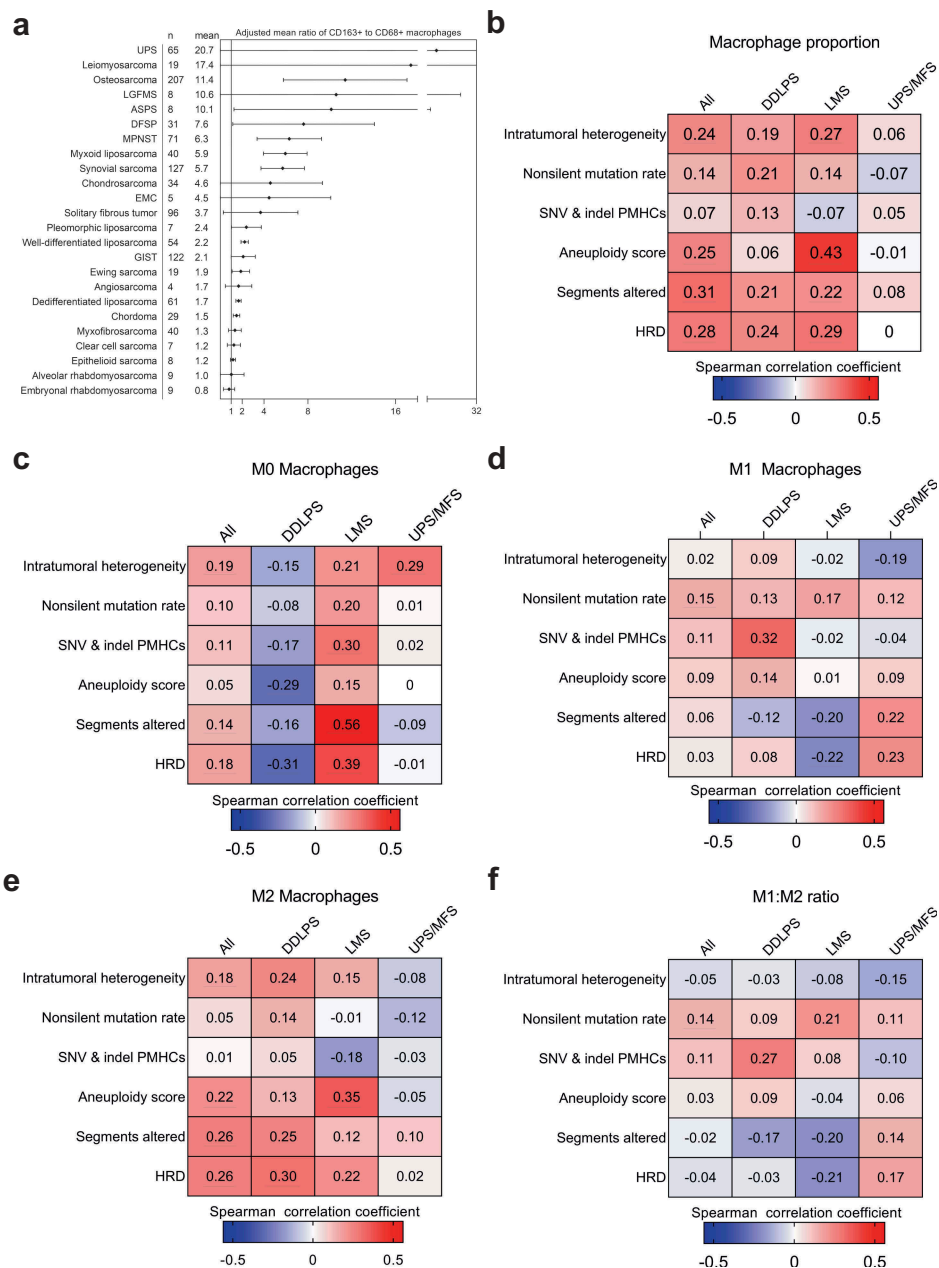
Figure 3. Macrophage polarization in sarcomas. (a) Adjusted mean ratio of CD163/CD68, based on counts of positive-staining immune cells per mm2 tumor tissue, scored from tissue microarray cores. Error bars represent 95% confidence interval of the mean. In order to avoid dividing by zero, all values were adjusted by adding $1/mm^2$ prior to calculating ratio. (b-f) Heatmaps display Spearman rank correlation coefficients for pleomorphic sarcoma types between indicated macrophage signatures (calculated as proportion of total immune infiltrate) and DNA damage measures calculated by Thorsson *et al.* (2018). Underlined values indicate statistically significant correlations (p ≤ 0.05). (b) Degree of association between relative macrophage proportion of immune infiltrates and measures of DNA damage. (c-e) Association between macrophage subsets, M0, M1, M2 with DNA damage. (f) Correlation between M1:M2 ratio and DNA damage measures. Abbreviations: ASPS, alveolar soft part sarcoma, DDLPS, dedifferentiated liposarcoma; DFSP, dermatofibrosarcoma protuberans; EMC, extraskeletal myxoid chondrosarcoma; GIST, gastrointestinal stromal tumor; HRD, homologous recombination deficiency; LMS, leiomyosarcoma; MFS, myxofibrosarcoma; MPNST, malignant peripheral nerve sheath tumor; SNV & indel pMHCs, predicted neoantigens resulting from single nucleotide and insertion/deletion mutations; UPS, undifferentiated pleomorphic sarcoma.

sarcoma (70% of cases negative for CD47) (Figure 4(b)). Notable high expressers of CD47 included chordoma and angiosarcoma, which demonstrated CD47 staining in all cases, with fully 100% of neoplastic cells expressing CD47 in 82% of chordomas and 75% of angiosarcomas. Pleomorphic and dedifferentiated liposarcomas and epithelioid sarcoma also exhibited high proportions of CD47 staining, with >90% of tumor cells expressing CD47 in 71%, 64%, and 63% of samples, respectively (Figure 4(b)).

Overall, at least one SIRPα+ macrophage was identified in 31.3% of cases. The sarcoma types most commonly infiltrated by SIRPα+ macrophages were dedifferentiated liposarcoma (77% of cases), angiosarcoma (75%), chordoma (71%), and well-differentiated liposarcoma (65%) (Figure 4(c)). SIRPα infiltration was least common in low-grade fibromyxoid sarcoma (0% of cases), chondrosarcoma (2%), epithelioid sarcoma (13%), and synovial sarcoma (14%) (Figure 4(c)). Of note, SIRPα expression was not confined to macrophages, but
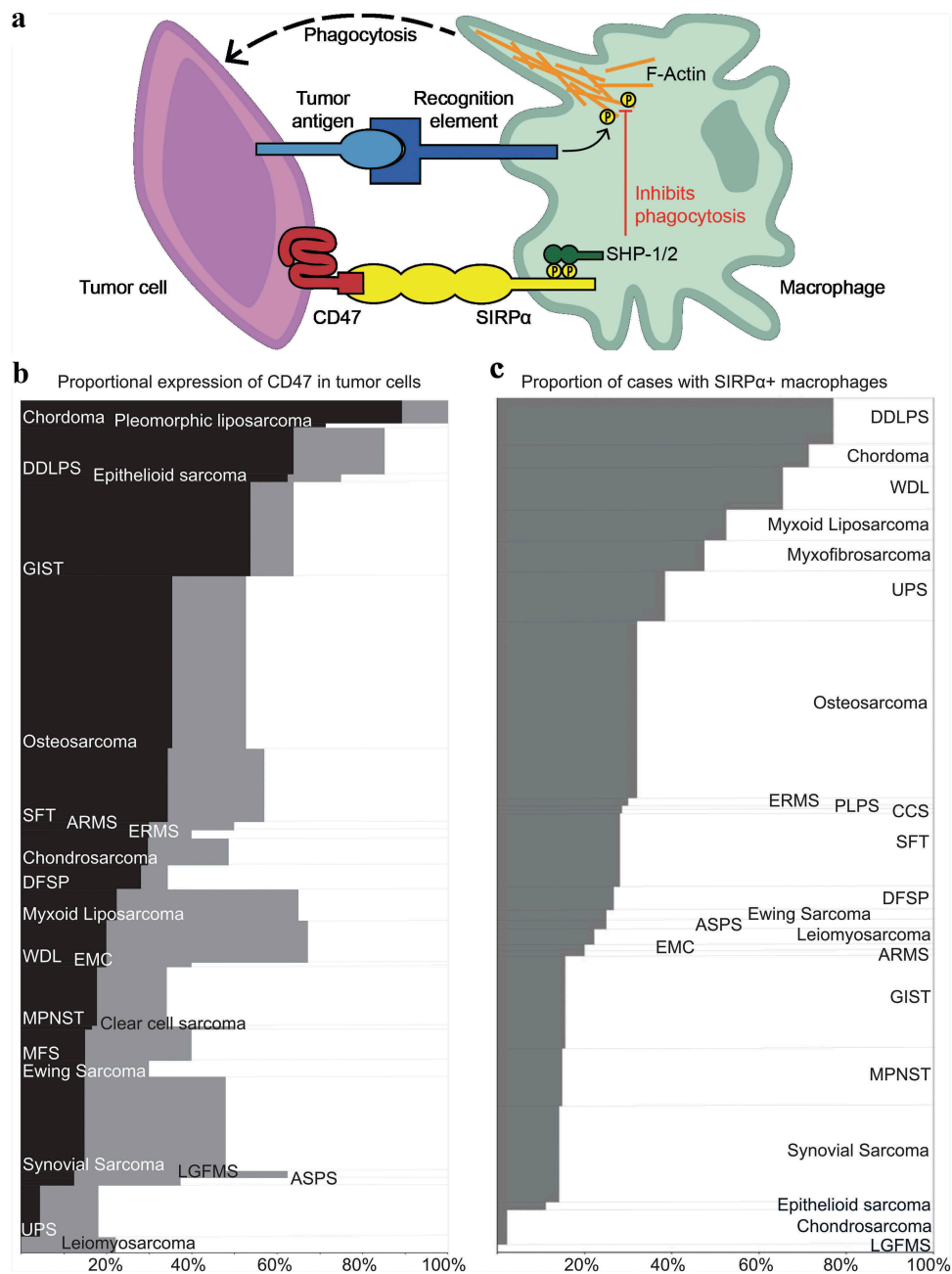
Figure 4. Macrophage-associated immune checkpoint CD47/SIRPα in sarcomas. (a) Schematic depicting mechanism of action of the CD47 self-recognition "don't eat me" immune checkpoint. Tumor-expressed CD47 ligand binds to SIRPα receptor on macrophages, inducing cytoplasmic tyrosine-phosphorylation. Phosphorylated SIRPα recruits and activates SH2-domain-containing tyrosine phosphatases SHP-1 and SHP-2, which in turn dephosphorylate specific protein substrates – such as F-Actin – thereby inhibiting phagocytosis. (b) Mosaic plot depicting the proportion of cases expressing CD47 (by immunohistochemistry) in 0% (white), 1–89% (gray), or 90–100% (black) of tumor cells. Column height is proportional to the number of cases assessed. Only sarcoma types with ≥5 cases available for analysis are shown. (c) Mosaic plot depicting the proportion of cases with at least 1 SIRPα+ macrophage (by immunohistochemistry; positive cases in gray) in any tissue microarray core. Only sarcoma types with ≥5 cases available for analysis are shown.

on occasion was seen in tumor cells (Table S5), most notably with 11/21 (52%) of Ewing sarcomas being positive for SIRPα in a variable membranous to granular cytoplasmic staining pattern. Frequent SIRPα expression in Ewing sarcoma was confirmed using a second independent tissue microarray showing tumor cell SIRPα expression in 18/38 (47%) of Ewing cases.

Across all sarcomas, tumor-associated macrophage expression of receptor SIRPα weakly correlated with tumor expression of CD47 ($r_S = 0.23$, $p < .0001$) (Figure S3A&B). Likewise, CD47 and

SIRPα expression showed weak positive correlations with both CD68 and CD163 across all sarcomas (Figure S3B), with only solitary fibrous tumor showing a significant negative correlation between CD47 and both CD163 and CD68 ($r_S = -0.32$, $p = .0045$, and $r_S = -0.45$, $p < .0001$, respectively; Figure S3B). SIRPα also correlated weakly with macrophage expression of PD-L1 across all sarcomas ($r_s = 0.24$, $p < .0001$), with significant positive correlations seen in myxofibrosarcoma, osteosarcoma, dedifferentiated liposarcoma, and synovial sarcoma ($p < .04$). SIRPα correlated poorly with most clinicopathologic tumor features, with more

frequent positivity only in higher grade myxofibrosarcoma ($p = .039$) in an exploratory analysis (Table S6A). CD47 was not significantly correlated with specific tumor clinicopathologic features (Table S6B).

Prognostic correlates

Multivariable Cox regression analyses were conducted for the non-translocation and for the translocation-associated sarcomas, taking into account patient age and immunohistochemical scores for CD68, CD163, CD47, and SIRPα as continuous variables, and tumor grade as low, intermediate-to-high, or unknown/not applicable (Table S7). Among the non-translocation sarcomas, age, grade, and lower SIRPα score were associated with worse overall survival (OS) ($p < .05$), while among the translocation-associated sarcomas only intermediate-to-high grade correlated with worse OS ($p = .04$). For progression-free survival (PFS), grade ($p = .04$) was associated with worse outcomes (Table S7) among non-translocation sarcomas, while lower CD47 score was associated with worse outcomes among translocation-associated sarcomas ($p = .03$; Table S7).

Univariable Cox proportional hazards models (Figure 5) were used to assess PFS in sarcoma types with at least 10 cases with clinical follow-up (Table S8). While the presence of any SIRPα+ macrophage was an adverse prognostic factor in both synovial sarcoma and myxofibrosarcoma (Figure 5(a,b)), the prognostic significance of CD47 and tumor-associated macrophages varied depending on tumor type (Figure 5(c,d)). CD47 expression was an adverse prognostic factor in osteosarcoma, but not in solitary fibrous tumor (Figure 5(d)). That said, in solitary fibrous tumors, high CD163 predicted inferior PFS (Figure 5(d)), but in dedifferentiated liposarcoma high CD163 was a positive prognostic indicator (Figure 5(d)). It is possible that the inverse correlation seen between CD47 and CD163 in solitary fibrous tumors may account for the different effects seen in the sarcoma type-specific contexts.

Discussion

With somewhat disappointing results emerging from immune checkpoint blockade trials targeting the adaptive immune response to sarcomas,[3-5] newer studies are turning to
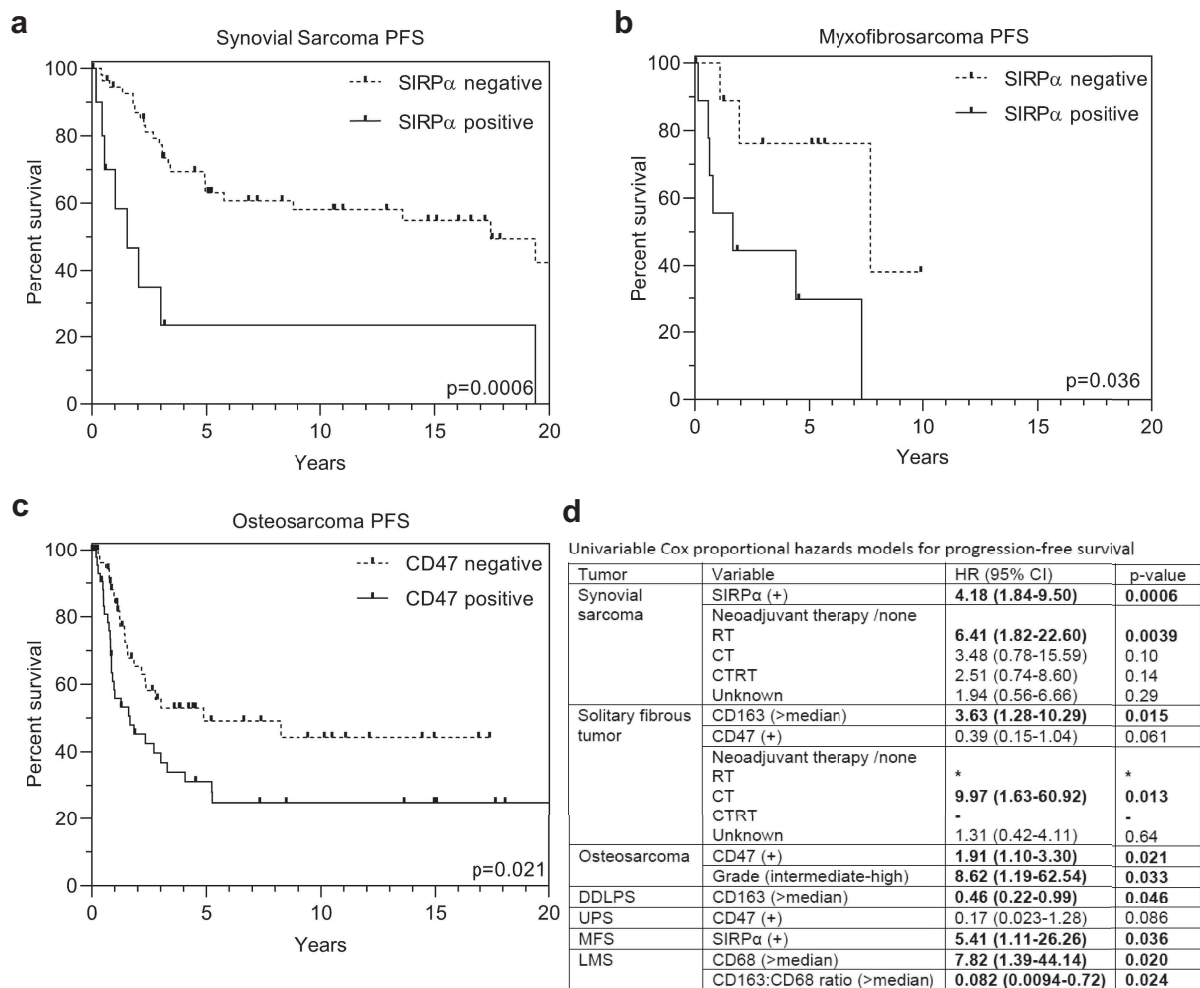
Figure 5. Prognostic implications of tumor-associated macrophage biomarkers in sarcomas, based on immunohistochemical staining of tissue microarrays. Kaplan–Meier curves (a-e) show Progression-free survival (PFS) based on any SIRPα-positivity in synovial sarcoma (a) and myxofibrosarcoma (b). (c) PFS based on any CD47-positivity in osteosarcoma. (d) Univariable Cox proportional hazards models results for sarcoma types indicated, showing all variables with $p < .1$. Bold font indicates significant $p < .05$. Abbreviations: CT, chemotherapy; CTRT, chemoradiation therapy; DDLPS, dedifferentiated liposarcoma; LMS, leiomyosarcoma; MFS, myxofibrosarcoma; RT, radiation therapy; UPS, undifferentiated pleomorphic sarcoma.

Univariable Cox proportional hazards models for progression-free survival

Tumor	Variable	HR (95% CI)	p-value
Synovial sarcoma	SIRPα (+)	**4.18 (1.84-9.50)**	**0.0006**
	Neoadjuvant therapy /none		
	RT	**6.41 (1.82-22.60)**	**0.0039**
	CT	3.48 (0.78-15.59)	0.10
	CTRT	2.51 (0.74-8.60)	0.14
	Unknown	1.94 (0.56-6.66)	0.29
Solitary fibrous tumor	CD163 (>median)	**3.63 (1.28-10.29)**	**0.015**
	CD47 (+)	0.39 (0.15-1.04)	0.061
	Neoadjuvant therapy /none		
	RT	*	*
	CT	**9.97 (1.63-60.92)**	**0.013**
	CTRT	-	-
	Unknown	1.31 (0.42-4.11)	0.64
Osteosarcoma	CD47 (+)	**1.91 (1.10-3.30)**	**0.021**
	Grade (intermediate-high)	**8.62 (1.19-62.54)**	**0.033**
DDLPS	CD163 (>median)	**0.46 (0.22-0.99)**	**0.046**
UPS	CD47 (+)	0.17 (0.023-1.28)	0.086
MFS	SIRPα (+)	**5.41 (1.11-26.26)**	**0.036**
LMS	CD68 (>median)	**7.82 (1.39-44.14)**	**0.020**
	CD163:CD68 ratio (>median)	**0.082 (0.0094-0.72)**	**0.024**

combinations with novel immune checkpoint inhibitors, including some that affect the innate immune response. The rational design of these trials requires a detailed understanding of the immune microenvironments among the diverse types of sarcomas. The innate and adaptive arms of the immune system work together in concert to perform cancer immunosurveillance and eliminate most nascent tumors. In clinically apparent tumors, the tumor cells have subverted the innate immune response, which includes macrophages, to promote tumorigenesis via cytokine and growth factor secretion. Understanding the balance between tumor-associated macrophages and TILs may better delineate the targetable mechanisms behind immune-evasion, specifically for each sarcoma type. Our study provides a systematic characterization of tumor-associated macrophages and macrophage-related immune checkpoint biomarker expression. To our knowledge, this is the largest study to date to characterize tumor-associated macrophages in sarcomas, and the first description of CD47 and SIRPα expression across sarcoma types.

Our study depicts a widely variable, highly sarcoma-type-specific expression of both CD68+ and CD163+ tumor-associated macrophages. Tumor-associated macrophages were most frequently observed in pleomorphic sarcomas, such as undifferentiated pleomorphic sarcoma and dedifferentiated liposarcoma, and were most sparse in translocation-associated sarcomas, including synovial sarcoma, myxoid liposarcoma, clear cell sarcoma, and low-grade fibromyxoid sarcoma. This suggests that pleomorphic sarcoma types are somehow triggering higher levels of phagocytic inflammation than translocation-associated sarcomas. Moreover, the macrophage density in pleomorphic sarcomas exceeds that of TILs we previously published from the same tissue set,[57] suggesting that macrophages dominate the immune microenvironment of sarcomas relative to lymphocytes.

Among macrophages, we found that M2-like (CD163+) macrophages were the predominant phenotype, which agrees with findings in melanoma,[60] non-small cell lung cancer,[61] and colorectal cancer.[59,62] The presence of large numbers of M2-like macrophages suggests a highly immunosuppressive tumor microenvironment, but due to the plasticity of tumor-associated macrophage polarization, this could represent anti-tumor immunity that is suppressed-but-poised for reactivation.[63] The M2-like macrophage predominance might be explained by tumor expression of the CD47 self-antigen stimulating SIRPα+ macrophages, as both were commonly seen in our sample set and were usually positively-correlated, albeit to different extents depending on tumor type. SIRPα signaling has been shown to modulate macrophage polarization in mice, suggesting that activation of SIRPα receptor shifts macrophage polarization toward M2.[64] High levels of CD47 expression have been shown to be an adverse prognostic factor in several lymphomas, ovarian cancer, and glioblastoma.[36] Similarly, we found that in osteosarcoma, myxofibrosarcoma, and synovial sarcoma, expression of either CD47 or the presence of SIRPα+ macrophages were adverse prognostic features, and moreover, we found that in both osteosarcoma and synovial sarcoma, CD47 and SIRPα levels correlated with higher CD68+ and CD163+ macrophage infiltrates, although not with each other. In contrast, high density of CD163+ macrophages showed highly variable outcome associations, being correlated with adverse outcomes in solitary fibrous tumor and improved outcomes in dedifferentiated liposarcoma, similar to a recent report finding positive prognostic correlation for high CD163+ macrophages in rhabdomyosarcoma.[18] Taken together, these findings suggest that it is the interactions between tumor cells and macrophages that affect sarcoma behavior, rather than the degree of macrophage infiltration alone.

In pre-clinical trials, anti-CD47/SIRPα blockade has shown an anti-tumor effect in a variety of human malignancies via de-repression of macrophage phagocytosis of tumor cells,[65,66] which in turn promotes the display of tumor neoantigens on antigen-presenting cells, helping to enhance the adaptive anti-tumor response.[67] Moreover, SIRPα has been reported to be expressed on tumor cells in some cases of renal cell carcinoma and melanoma, and in these tumors, SIRPα/CD47 blockade using an anti SIRPα antibody may also directly induce cellular phagocytosis via opsonization.[66] Early clinical trials with CD47/SIRPα axis inhibitors have shown promising activity in B-cell lymphoma and some solid tumors.[40–42,66] Our findings, demonstrating frequent expression of CD47 in many sarcomas, suggest that targeting the CD47/SIRPα axis in these tumors may be worthwhile, for example, in chordoma and dedifferentiated liposarcoma. However, it should be noted that some relatively common sarcoma types (including leiomyosarcoma, undifferentiated pleomorphic sarcoma, and Ewing sarcoma) expressed CD47 infrequently, reiterating the potential for false-negative results when trials lump together different soft tissue sarcomas. Moreover, Ewing sarcoma cells expressed SIRPα in approximately 50% of cases, suggesting that this receptor may serve an alternate function in Ewing sarcoma and raising the possibility that CD47-blockade may have different effects in this context, although directly targeting SIRPα could be considered, as suggested by Yanagita et al. (2017).[66]

Our findings have significant limitations. Small numbers were available of some sarcoma types, and tissue microarray specimens do not take into account intratumoral heterogeneity or immune infiltrates near the tumor margins. However, tissue microarrays represent diagnostic core needle biopsy specimens reasonably well[68] and infiltrates were measured by cells/mm^2 to reflect this. Disagreement exists regarding the immunohistochemical identification of M1-like versus M2-like macrophages. Some studies choose to define CD68 as a general macrophage marker, back-calculating M1 macrophages as CD68 minus CD163.[60,69] However, others have shown that CD68 tends to underestimate the total macrophage count.[70] In our sample set, CD68 scores were lower than CD163 scores, indicating that CD68 was not staining all macrophages. We therefore defined CD68 as staining M1-like macrophages, although we recognize that this represents an imperfect, simplified model.

In order to provide further support for our observations, we used detailed RNA expression data from TCGA to model macrophage expression signatures. Deconvolution algorithms, such as CIBERSORT (used in the analysis of immune subtypes across all TCGA tumors)[71] attempt to extract proportionate cell populations based on known gene signatures. While this approach has its own limitations, we found that in general the RNA data supported our immunohistochemical findings, showing that macrophages comprised a median of 56% of the immune cell infiltrates among leiomyosarcoma, undifferentiated pleomorphic sarcoma, myxofibrosarcoma, and dedifferentiated liposarcoma, with a median macrophage:lymphocyte ratio of 1.7,[58] and that M2 macrophages

represented a larger component of the immune infiltrate than either M0 or M1.

We noted an association between measures of DNA damage and the composition of immune infiltrates. The relative macrophage fraction seen in sarcomas correlated with increased intratumoral heterogeneity, aneuploidy score, focal chromosomal copy number alterations, and homologous recombination defects (with the strongest associations seen in leiomyosarcoma). A possible explanation for this association could be that DNA damage can upregulate the expression of damage-associated molecular patterns (DAMPs), which promote inflammation, particularly from macrophages[72] and, more specifically, M2-polarized macrophages.[73,74] Alternatively, while rapidly-growing tumors accumulate DNA damage, they also outgrow their blood supply, leaving behind necrotic tissue, which in turn attracts macrophages.

In conclusion, we present the largest study to date of tumor-associated macrophage biomarkers in sarcomas. We observe a very high density of tumor-associated macrophages relative to tumor-infiltrating lymphocytes, and that these are predominately M2-like. We also observed frequent expression of the innate immunity checkpoint CD47 – particularly among angiosarcoma, chordoma, pleomorphic and dedifferentiated liposarcoma, and epithelioid sarcoma – suggesting that these sarcoma subtypes are most worthy candidates for anti-CD47 therapies, possibly in combination with adaptive immune checkpoint inhibition strategies, which are already providing evidence of activity in some of these sarcoma subtypes.

Acknowledgments

Disclosure of Potential Conflicts of Interest

The authors report no conflict of interest.

Funding

ORCID

Jean-Yves Blay ⓘ http://orcid.org/0000-0001-7190-120X

References

1. Fletcher CDM, Bridge JA, Hogendoorn P, Mertens C, eds. WHO classification of tumours of soft tissue and bone. 4th ed. Lyon: IARC Press, Bordeaux, France; 2013. IARC WHO Classification of Tumours; No. 5.

2. Coley WB II. Contribution to the knowledge of sarcoma. Ann Surg. 1891;14(3):199–220. doi:10.1097/00000658-189112000-00015.

3. Tawbi HA, Burgess M, Bolejack V, Van Tine BA, Schuetze SM, Hu J, D'Angelo S, Attia S, Riedel RF, Priebat DA, et al. Pembrolizumab in advanced soft-tissue sarcoma and bone sarcoma (SARC028): a multicentre, two-cohort, single-arm, open-label, phase 2 trial. Lancet Oncol. 2017;18(11):1493–1501. doi:10.1016/S1470-2045(17)30624-1.

4. D'Angelo SP, Mahoney MR, Van Tine BA, Atkins J, Milhem MM, Jahagirdar BN, Antonescu CR, Horvath E, Tap WD, Schwartz GK, et al. Nivolumab with or without ipilimumab treatment for metastatic sarcoma (Alliance A091401): two open-label, non-comparative, randomised, phase 2 trials. Lancet Oncol. 2018;19(3):416–426. doi:10.1016/S1470-2045(18)30006-8.

5. Toulmonde M, Penel N, Adam J, Chevreau C, Blay J-Y, Le Cesne A, Bompas E, Piperno-Neumann S, Cousin S, Grellety T, et al. Use of PD-1 targeting, macrophage infiltration, and IDO pathway activation in sarcomas: a phase 2 clinical trial. JAMA Oncol. 2018;4(1):93–97. doi:10.1001/jamaoncol.2017.1617.

6. Gide TN, Wilmott JS, Scolyer RA, Long GV. Primary and acquired resistance to immune checkpoint inhibitors in metastatic melanoma. Clin Cancer Res. 2018;24(6):1260–1270. doi:10.1158/1078-0432.CCR-17-2267.

7. Mantovani A, Bottazzi B, Colotta F, Sozzani S, Ruco L. The origin and function of tumor-associated macrophages. Immunol Today. 1992;13(7):265–270. doi:10.1016/0167-5699(92)90008-U.

8. Atri C, Guerfali FZ, Laouini D. Role of human macrophage polarization in inflammation during infectious diseases. Int J Mol Sci. 2018;19(6):1801. doi:10.3390/ijms19061801.

9. Mackaness GB. The immunological basis of acquired cellular resistance. J Exp Med. 1964;120:105–120. doi:10.1084/jem.120.1.105.

10. Mantovani A, Sica A, Sozzani S, Allavena P, Vecchi A, Locati M. The chemokine system in diverse forms of macrophage activation and polarization. Trends Immunol. 2004;25(12):677–686. doi:10.1016/j.it.2004.09.015.

11. Biswas SK, Mantovani A. Macrophage plasticity and interaction with lymphocyte subsets: cancer as a paradigm. Nat Immunol. 2010;11(10):889–896. doi:10.1038/ni.1937.

12. Tarique AA, Logan J, Thomas E, Holt PG, Sly PD, Fantino E. Phenotypic, functional, and plasticity features of classical and alternatively activated human macrophages. Am J Respir Cell Mol Biol. 2015;53(5):676–688. doi:10.1165/rcmb.2015-0012OC.

13. Duluc D, Corvaisier M, Blanchard S, Catala L, Descamps P, Gamelin E, Ponsoda S, Delneste Y, Hebbar M, Jeannin P, et al. Interferon-gamma reverses the immunosuppressive and protumoral properties and prevents the generation of human tumor-associated macrophages. Int J Cancer. 2009;125(2):367–373. doi:10.1002/ijc.24401.

14. Guiducci C, Vicari AP, Sangaletti S, Trinchieri G, Colombo MP. Redirecting in vivo elicited tumor infiltrating macrophages and dendritic cells towards tumor rejection. Cancer Res. 2005;65(8):3437–3446. doi:10.1158/0008-5472.CAN-04-4262.

15. Bingle L, Brown NJ, Lewis CE. The role of tumour-associated macrophages in tumour progression: implications for new anticancer therapies. J Pathol. 2002;196(3):254–265. doi:10.1002/path.1027.

16. Zhang QW, Liu L, Gong CY, Shi H-S, Zeng Y-H, Wang X-Z, Zhao Y-W, Wei Y-Q. Prognostic significance of tumor-associated macrophages in solid tumor: a meta-analysis of the literature. PLoS One. 2012;7(12):e50946. doi:10.1371/journal.pone.0050946.

17. D'Angelo SP, Shoushtari AN, Agaram NP, Kuk D, Qin L-X, Carvajal RD, Dickson MA, Gounder M, Keohan ML, Schwartz GK, et al. Prevalence of tumor-infiltrating lymphocytes and PD-L1 expression in the soft tissue sarcoma microenvironment. Hum Pathol. 2015;46(3):357–365. doi:10.1016/j.humpath.2014.11.001.

18. Kather JN, Horner C, Weis CA, Aung T, Vokuhl C, Weiss C, Scheer M, Marx A, Simon-Keller K. CD163+ immune cell infiltrates and presence of CD54+ microvessels are prognostic markers for patients with embryonal rhabdomyosarcoma. Sci Rep. 2019;9(1):9211. doi:10.1038/s41598-019-45551-y.

19. Bindea G, Mlecnik B, Tosolini M, Kirilovsky A, Waldner M, Obenauf A, Angell H, Fredriksen T, Lafontaine L, Berger A, et al. Spatiotemporal dynamics of intratumoral immune cells reveal the immune landscape in human cancer. Immunity. 2013;39(4):782–795. doi:10.1016/j.immuni.2013.10.003.

20. The Cancer Genome Atlas Research Network. Comprehensive and integrated genomic characterization of adult soft tissue sarcomas. Cell. 2017;171(4):950–965 e928. doi:10.1016/j.cell.2017.10.014.

21. Lee CH, Espinosa I, Vrijaldenhoven S, Subramanian S, Montgomery KD, Zhu S, Marinelli RJ, Peterse JL, Poulin N, Nielsen TO, et al. Prognostic significance of macrophage infiltration in leiomyosarcomas. Clin Cancer Res. 2008;14(5):1423–1430. doi:10.1158/1078-0432.CCR-07-1712.

22. Ganjoo KN, Witten D, Patel M, Espinosa I, La T, Tibshirani R, van de Rijn M, Jacobs C, West RB. The prognostic value of tumor-associated macrophages in leiomyosarcoma: a single institution study. Am J Clin Oncol. 2011;34(1):82–86. doi:10.1097/COC.0b013e3181d26d5e.

23. George S, Miao D, Demetri GD, Adeegbe D, Rodig SJ, Shukla S, Lipschitz M, Amin-Mansour A, Raut CP, Carter SL, et al. Loss of PTEN is associated with resistance to anti-PD-1 checkpoint blockade therapy in metastatic uterine leiomyosarcoma. Immunity. 2017;46(2):197–204. doi:10.1016/j.immuni.2017.02.001.

24. Reinhold MI, Lindberg FP, Plas D, Reynolds S, Peters MG, Brown EJ. In vivo expression of alternatively spliced forms of integrin-associated protein (CD47). J Cell Sci. 1995;108:3419–3425.

25. Oldenborg PA, Zheleznyak A, Fang YF, Lagenaur CF, Gresham HD, Lindberg FP. Role of CD47 as a marker of self on red blood cells. Science. 2000;288(5473):2051–2054. doi:10.1126/science.288.5473.2051.

26. Fossati-Jimack L, Azeredo da Silveira S, Moll T, Kina T, Kuypers FA, Oldenborg P-A, Reininger L, Izui S, Azeredo da Silveira S, Moll T, et al. Selective increase of autoimmune epitope expression on aged erythrocytes in mice: implications in anti-erythrocyte autoimmune responses. J Autoimmun. 2002;18(1):17–25. doi:10.1006/jaut.2001.0563.

27. Khandelwal S, van Rooijen N, Saxena RK. Reduced expression of CD47 during murine red blood cell (RBC) senescence and its role in RBC clearance from the circulation. Transfusion. 2007;47(9):1725–1732. doi:10.1111/j.1537-2995.2007.01348.x.

28. Olsson M, Nilsson A, Oldenborg PA. Dose-dependent inhibitory effect of CD47 in macrophage uptake of IgG-opsonized murine erythrocytes. Biochem Biophys Res Commun. 2007;352(1):193–197. doi:10.1016/j.bbrc.2006.11.002.

29. Ishikawa-Sekigami T, Kaneko Y, Okazawa H, Tomizawa T, Okajo J, Saito Y, Okuzawa C, Sugawara-Yokoo M, Nishiyama U, Ohnishi H, et al. SHPS-1 promotes the survival of circulating erythrocytes through inhibition of phagocytosis by splenic macrophages. Blood. 2006;107(1):341–348. doi:10.1182/blood-2005-05-1896.

30. Yamao T, Noguchi T, Takeuchi O, Nishiyama U, Morita H, Hagiwara T, Akahori H, Kato T, Inagaki K, Okazawa H, et al. Negative regulation of platelet clearance and of the macrophage phagocytic response by the transmembrane glycoprotein SHPS-1. J Biol Chem. 2002;277(42):39833–39839. doi:10.1074/jbc.M203287200.

31. Fujioka Y, Matozaki T, Noguchi T, Iwamatsu A, Yamao T, Takahashi N, Tsuda M, Takada T, Kasuga M. A novel membrane glycoprotein, SHPS-1, that binds the SH2-domain-containing protein tyrosine phosphatase SHP-2 in response to mitogens and cell adhesion. Mol Cell Biol. 1996;16(12):6887–6899. doi:10.1128/MCB.16.12.6887.

32. Jaiswal S, Jamieson CH, Pang WW, Park CY, Chao MP, Majeti R, Traver D, van Rooijen N, Weissman IL. CD47 is upregulated on circulating hematopoietic stem cells and leukemia cells to avoid phagocytosis. Cell. 2009;138(2):271–285. doi:10.1016/j.cell.2009.05.046.

33. Chan KS, Espinosa I, Chao M, Wong D, Ailles L, Diehn M, Gill H, Presti J, Chang HY, van de Rijn M, et al. Identification, molecular characterization, clinical prognosis, and therapeutic targeting of human bladder tumor-initiating cells. Proc Natl Acad Sci USA. 2009;106(33):14016–14021. doi:10.1073/pnas.0906549106.

34. Chao MP, Alizadeh AA, Tang C, Myklebust JH, Varghese B, Gill S, Jan M, Cha AC, Chan CK, Tan BT, et al. Anti-CD47 antibody synergizes with rituximab to promote phagocytosis and eradicate non-Hodgkin lymphoma. Cell. 2010;142(5):699–713. doi:10.1016/j.cell.2010.07.044.

35. Edris B, Weiskopf K, Volkmer AK, Volkmer J-P, Willingham SB, Contreras-Trujillo H, Liu J, Majeti R, West RB, Fletcher JA, et al. Antibody therapy targeting the CD47 protein is effective in a model of aggressive metastatic leiomyosarcoma. Proc Natl Acad Sci USA. 2012;109(17):6656–6661. doi:10.1073/pnas.1121629109.

36. Willingham SB, Volkmer JP, Gentles AJ, Sahoo D, Dalerba P, Mitra SS, Wang J, Contreras-Trujillo H, Martin R, Cohen JD, et al. The CD47-signal regulatory protein alpha (SIRPa) interaction is a therapeutic target for human solid tumors. Proc Natl Acad Sci USA. 2012;109(17):6662–6667. doi:10.1073/pnas.1121623109.

37. Majeti R, Chao MP, Alizadeh AA, Pang WW, Jaiswal S, Gibbs KD, van Rooijen N, Weissman IL. CD47 is an adverse prognostic factor and therapeutic antibody target on human acute myeloid leukemia stem cells. Cell. 2009;138(2):286–299. doi:10.1016/j.cell.2009.05.045.

38. Xiao Z, Chung H, Banan B, Manning PT, Ott KC, Lin S, Capoccia BJ, Subramanian V, Hiebsch RR, Upadhya GA, et al. Antibody mediated therapy targeting CD47 inhibits tumor progression of hepatocellular carcinoma. Cancer Lett. 2015;360(2):302–309. doi:10.1016/j.canlet.2015.02.036.

39. Liu J, Wang L, Zhao F, Tseng S, Narayanan C, Shura L, Willingham S, Howard M, Prohaska S, Volkmer J, et al. Pre-clinical development of a humanized anti-CD47 antibody with anti-cancer therapeutic potential. PLoS One. 2015;10(9):e0137345. doi:10.1371/journal.pone.0137345.

40. Advani R, Flinn I, Popplewell L, Forero A, Bartlett NL, Ghosh N, Kline J, Roschewski M, LaCasce A, Collins GP, et al. CD47 blockade by Hu5F9-G4 and rituximab in non-hodgkin's lymphoma. N Engl J Med. 2018;379(18):1711–1721. doi:10.1056/NEJMoa1807315.

41. Sikic BI, Lakhani N, Patnaik A, Shah SA, Chandana SR, Rasco D, Colevas AD, O'Rourke T, Narayanan S, Papadopoulos K, et al. First-in-human, first-in-class phase i trial of the anti-CD47 antibody Hu5F9-G4 in patients with advanced cancers. J Clin Oncol. 2019;37(12):946–953. doi:10.1200/JCO.18.02018.

42. Ansell S, Chen RW, Flinn IW, Maris MB, O'Connor OA, Johnson LD, Irwin M, Petrova PS, Uger RA, Sievers EL, et al. A phase 1 study of TTI-621, a novel immune checkpoint inhibitor targeting CD47, in patients with relapsed or refractory hematologic malignancies. Blood. 2016;128(22):1812. doi:10.1182/blood.V128.22.1812.1812.

43. Manna PP, Frazier WA. CD47 mediates killing of breast tumor cells via Gi-dependent inhibition of protein kinase A. Cancer Res. 2004;64(3):1026–1036. doi:10.1158/0008-5472.CAN-03-1708.

44. Rendtlew Danielsen JM, Knudsen LM, Dahl IM, Lodahl M, Rasmussen T. Dysregulation of CD47 and the ligands thrombospondin 1 and 2 in multiple myeloma. Br J Haematol. 2007;138(6):756–760. doi:10.1111/j.1365-2141.2007.06729.x.

45. Kim MJ, Lee JC, Lee JJ, Kim S, Lee SG, Park S-W, Sung MW, Heo DS. Association of CD47 with natural killer cell-mediated cytotoxicity of head-and-neck squamous cell carcinoma lines. Tumour Biol. 2008;29(1):28–34. doi:10.1159/000132568.

46. Xu JF, Pan XH, Zhang SJ, Zhao C, Qiu B-S, Gu H-F, Hong J-F, Cao L, Chen Y, Xia B, et al. CD47 blockade inhibits tumor progression human osteosarcoma in xenograft models. Oncotarget. 2015;6(27):23662–23670. doi:10.18632/oncotarget.4282.

47. Nielsen TO, Hsu FD, O'Connell JX, Gilks CB, Sorensen PHB, Linn S, West RB, Liu CL, Botstein D, Brown PO, et al. Tissue microarray validation of epidermal growth factor receptor and SALL2 in synovial sarcoma with comparison to tumors of similar histology. Am J Pathol. 2003;163(4):1449–1456. doi:10.1016/S0002-9440(10)63502-X.

48. Ng TL, Gown AM, Barry TS, Cheang MCU, Chan AKW, Turbin DA, Hsu FD, West RB, Nielsen TO. Nuclear beta-catenin in mesenchymal tumors. Mod Pathol. 2005;18 (1):68–74. doi:10.1038/modpathol.3800272.

49. Steigen SE, Straume B, Turbin D, Chan AKW, Leung S, Nielsen TO, Lindal S. Clinicopathologic factors and nuclear morphometry as independent prognosticators in KIT-positive gastrointestinal stromal tumors. J Histochem Cytochem. 2008;56 (2):139–145. doi:10.1369/jhc.7A7333.2007.

50. Cheng H, Dodge J, Mehl E, Liu S, Poulin N, van de Rijn M, Nielsen TO. Validation of immature adipogenic status and identification of prognostic biomarkers in myxoid liposarcoma using tissue microarrays. Hum Pathol. 2009;40(9):1244–1251. doi:10.1016/j.humpath.2009.01.011.

51. Pacheco M, Nielsen TO. Histone deacetylase 1 and 2 in mesenchymal tumors. Mod Pathol. 2012;25(2):222–230. doi:10.1038/modpathol.2011.157.

52. Endo M, Su L, Nielsen TO. Activating transcription factor 2 in mesenchymal tumors. Hum Pathol. 2014;45(2):276–284. doi:10.1016/j.humpath.2013.09.003.

53. Endo M, de Graaff MA, Ingram DR, Lim S, Lev DC, Briaire-de Bruijn IH, Somaiah N, Bovée JV, Lazar AJ, Nielsen TO, et al. NY-ESO-1 (CTAG1B) expression in mesenchymal tumors. Mod Pathol. 2015;28(4):587–595. doi:10.1038/modpathol.2014.155.

54. Banito A, Li X, Laporte AN, Roe J-S, Sanchez-Vega F, Huang C-H, Dancsok AR, Hatzi K, Chen -C-C, Tschaharganeh DF, et al. The SS18-SSX oncoprotein Hijacks KDM2B-PRC1.1 to drive synovial sarcoma. Cancer Cell. 2018;33 (3):527–541 e528. doi:10.1016/j.ccell.2018.01.018.

55. Terry J, Saito T, Subramanian S, Ruttan C, Antonescu CR, Goldblum JR, Downs-Kelly E, Corless CL, Rubin BP, van de Rijn M, et al. TLE1 as a diagnostic immunohistochemical marker for synovial sarcoma emerging from gene expression profiling studies. Am J Surg Pathol. 2007;31(2):240–246. doi:10.1097/01.pas.0000213330.71745.39.

56. Demicco EG, Harms PW, Patel RM, Smith SC, Ingram D, Torres K, Carskadon SL, Camelo-Piragua S, McHugh JB, Siddiqui J, et al. Extensive survey of STAT6 expression in a large series of mesenchymal tumors. Am J Clin Pathol. 2015;143(5):672–682. doi:10.1309/AJCPN25NJTOUNPNF.

57. Dancsok AR, Setsu N, Gao D, Blay J-Y, Thomas D, Maki RG, Nielsen TO, Demicco EG. Expression of lymphocyte immunoregulatory biomarkers in bone and soft-tissue sarcomas. Mod Pathol. 2019;32(12):1772–1785. doi:10.1038/s41379-019-0312-y.

58. Thorsson V, Gibbs DL, Brown SD, Wolf D, Bortone DS, Ou Yang T-H, Porta-Pardo E, Gao GF, Plaisier CL, Eddy JA, et al. The immune landscape of cancer. Immunity. 2018;48(4):812–830. e814. doi:10.1016/j.immuni.2018.03.023.

59. Edin S, Wikberg ML, Dahlin AM, Rutegård J, Öberg Å, Oldenborg P-A, Palmqvist R. The distribution of macrophages with a M1 or M2 phenotype in relation to prognosis and the molecular characteristics of colorectal cancer. PLoS One. 2012;7 (10):e47045. doi:10.1371/journal.pone.0047045.

60. Herwig MC, Bergstrom C, Wells JR, Holler T, Grossniklaus HE. M2/M1 ratio of tumor associated macrophages and PPAR-gamma expression in uveal melanomas with class 1 and class 2 molecular profiles. Exp Eye Res. 2013;107:52–58. doi:10.1016/j.exer.2012.11.012.

61. Jackute J, Zemaitis M, Pranys D, Sitkauskiene B, Miliauskas S, Vaitkiene S, Sakalauskas R. Distribution of M1 and M2 macrophages in tumor islets and stroma in relation to prognosis of non-small cell lung cancer. BMC Immunol. 2018;19(1):3. doi:10.1186/s12865-018-0241-4.

62. Yahaya MAF, Lila MAM, Ismail S, Zainol M, Afizan N. Tumour-Associated Macrophages (TAMs) in colon cancer and how to reeducate them. J Immunol Res. 2019;2019:2368249. doi:10.1155/2019/2368249.

63. Zheng X, Turkowski K, Mora J, Brüne B, Seeger W, Weigert A, Savai R. Redirecting tumor-associated macrophages to become tumoricidal effectors as a novel strategy for cancer therapy. Oncotarget. 2017;8(29):48436–48452. doi:10.18632/oncotarget.17061.

64. Shi L, Bian Z, Liu Y. Dual role of SIRPÎ± in macrophage activation: inhibiting M1 while promoting M2 polarization via selectively activating SHP-1 and SHP-2 signal. J Immunol. 2017;198:67.12.

65. Yu XY, Qiu WY, Long F, Yang X-P, Zhang C, Xu L, Chang H-Y, Du P, Hou X-J, Yu Y-Z, et al. A novel fully human anti-CD47 antibody as a potential therapy for human neoplasms with good safety. Biochimie. 2018;151:54–66. doi:10.1016/j.biochi.2018.05.019.

66. Yanagita T, Murata Y, Tanaka D, Motegi S-I, Arai E, Daniwijaya EW, Hazama D, Washio K, Saito Y, Kotani T, et al. Anti-SIRPalpha antibodies as a potential new tool for cancer immunotherapy. JCI Insight. 2017;2(1):e89140. doi:10.1172/jci.insight.89140.

67. Chowdhury S, Castro S, Coker C, Hinchliffe TE, Arpaia N, Danino T. Programmable bacteria induce durable tumor regression and systemic antitumor immunity. Nat Med. 2019;25 (7):1057–1063. doi:10.1038/s41591-019-0498-z.

68. Voduc D, Kenney C, Nielsen TO. Tissue microarrays in clinical oncology. Semin Radiat Oncol. 2008;18(2):89–97. doi:10.1016/j.semradonc.2007.10.006.

69. Cornelissen R, Lievense LA, Maat AP, Hendriks RW, Hoogsteden HC, Bogers AJ, Hegmans JP, Aerts JG. Ratio of intratumoral macrophage phenotypes is a prognostic factor in epithelioid malignant pleural mesothelioma. PLoS One. 2014;9 (9):e106742. doi:10.1371/journal.pone.0106742.

70. Barros MH, Hauck F, Dreyer JH, Kempkes B, Niedobitek G. Macrophage polarisation: an immunohistochemical approach for identifying M1 and M2 macrophages. PLoS One. 2013;8: e80908.

71. Newman AM, Liu CL, Green MR, Gentles AJ, Feng W, Xu Y, Hoang CD, Diehn M, Alizadeh AA. Robust enumeration of cell subsets from tissue expression profiles. Nat Methods. 2015;12 (5):453–457. doi:10.1038/nmeth.3337.

72. Land WG. The role of damage-associated molecular patterns in human diseases: part i - promoting inflammation and immunity. Sultan Qaboos Univ Med J. 2015;15:e9–e21.

73. Hernandez C, Huebener P, Schwabe RF. Damage-associated molecular patterns in cancer: a double-edged sword. Oncogene. 2016;35(46):5931–5941. doi:10.1038/onc.2016.104.

74. He Y, Zha J, Wang Y, Liu W, Yang X, Yu P. Tissue damage-associated "danger signals" influence T-cell responses that promote the progression of preneoplasia to cancer. Cancer Res. 2013;73(2):629–639. doi:10.1158/0008-5472.CAN-12-2704.